small method
www.small-methods.com

MOFs for Electrocatalysis: From Serendipity to Design Strategies

*Harshitha Barike Aiyappa, Justus Masa, Corina Andronescu, Martin Muhler, Roland A. Fischer, and Wolfgang Schuhmann**

The rapid upsurge of metal–organic frameworks (MOFs) as well as MOF-derived materials has stimulated profound interest to capitalize on their many potential untapped benefits in electrocatalysis for energy applications. The possibility of tuning the metal–ligand junctions of the MOF architecture opens new avenues to design robust, extended heterostructures for addressing the present-day energy challenges. Interestingly, despite having detailed crystallographic information, it is often difficult to envisage the interplay of charge transport (electrons and ions), mass transport (pore system) together with the specific effects of the molecularly defined reaction center of MOFs for a given electrocatalytic reaction. Here, guidelines are offered for judiciously engineering the electronic structure of MOFs to deliver targeted electrocatalytic function. Some of the pivotal works on MOF-based materials for electrocatalysis are discussed, which can be correlated to the biological models in terms of their structural resemblance and an instructive insight is provided about the "new chemistry" that can be explored based on the lessons learned from nature in combination with the theoretical understanding of the energetics of the reactions.

1. Introduction

In a bid to address the growing global energy needs and simultaneously tackle the perils and the challenges associated with the present-day energy systems, the past decade has witnessed a revolution aiming to reduce the society's traditional dependence on exhaustible fossil resources. Specifically, the focus has relentlessly shifted toward sustainable energy provision by means of interconversion of chemical and electrical energy. This development has motivated the exploration of efficient alternatives to the conventionally used high cost and scarce electrocatalysts like Pt for the oxygen reduction reaction (ORR) or the hydrogen evolution reaction (HER), as well as RuO_2 and IrO_2 for the oxygen evolution reaction (OER), that are primarily involved in important electrochemical energy systems such as fuel cells, water electrolyzers, metal–air batteries, etc.[1–3] Specifically, the sluggish reaction kinetics associated with the oxygen electrochemical processes have necessitated a lookout for more efficient ORR and OER electrocatalysts, which can be economically implemented for large-scale applications. Any electrochemical reaction involving coupled diffusion–reaction–conduction processes typically encompasses the interactions between a solid electrode, an electrolyte, and the dissolved reactants or products. Ideally, such interactions demand the need for high electric and ionic conductivity apart from a high surface area interface to ensure the effective interaction between the different phases involved in these reactions.[4] A classic catalyst design strategy would target improving the quality (in terms of the intrinsic activity) and quantity (in terms of the density) of the active sites. Additionally, availability of large specific surface area with substantial porosity and high charge transfer capability are the prerequisites of the "ideal" electrocatalyst architecture. In this direction, a plethora of materials including carbon allotropes,[5] metal chalcogenides,[6] organometallic complexes,[7] conducting polymers[8] and their composites have been tested for their electrocatalytic activity. A recent class of porous materials, popularly known as metal–organic frameworks (MOFs) or porous coordination polymers (PCPs) have been extensively explored as electrocatalysts or as precursors to derive efficient heterostructures owing to their synthetic flexibility besides customizable electronic and chemical properties.[9–12] These highly crystalline materials are well known for their ultrahigh specific surface area of up to 10 000 $m^2\ g^{-1}$, wide pore size distribution, modifiable framework composition, and controllable pore volumes. The possibility to employ different metal ions-ligand coordination combinations with varying degrees of connectivity has stimulated the realization of ≈20 000 MOF

Dr. H. B. Aiyappa, Dr. J. Masa, Dr. C. Andronescu, Prof. W. Schuhmann
Analytical Chemistry – Center for Electrochemical Sciences (CES)
Faculty of Chemistry and Biochemistry
Ruhr University Bochum
Universitätstrasse 150, D-44780 Bochum, Germany
E-mail: wolfgang.schuhmann@rub.de
Prof. M. Muhler
Industrial Chemistry
Faculty of Chemistry and Biochemistry
Ruhr University Bochum
Universitätstrasse 150, D-44780 Bochum, Germany
Prof. R. A. Fischer
Department of Chemistry and Catalysis Research Centre
Technical University of Munich
85748 Garching, Germany
The ORCID identification number(s) for the author(s) of this article can be found under https://doi.org/10.1002/smtd.201800415.

DOI: 10.1002/smtd.201800415

structures to date, a figure which continues to grow.[13] From an electrochemical perspective, MOFs could be perceived as spatial architectures wherein discrete functional units can be designed to lie in close proximity so as to render sites for instigating bond breaking/forming reactions.[14] In particular, considering their highly accessible metal–ligand junctions, MOFs have been extensively tested for their interfacial electronic coupling interactions, which determine the efficiency of important electrochemical reactions involved in formation and splitting of water.[15] The high density of such closely located sites could consequently allow the reactants to easily navigate along the free energy landscape and transform into the desired products. The interaction energies between reactant, catalyst, and the product are the common descriptors that are believed to dictate the rate of these reactions. Thus, a rational combination of redox active metal ions and organic linkers offers a very convenient means of connecting essential electroactive components into infinite structural networks with desirable electrochemical functionality. If realized effectively, these predetermined catalytic sites could also be intelligently ordered to selectively drive cascaded reactions of vital electrochemical conversions involved, e.g., in the complex CO_2 reduction reaction (CO_2RR), which demands multifunctional catalytic sites for yielding products with high selectivity and specificity.[16] However, it is important to admit that despite numerous attempts to mimic biological catalytic sites, the synthetic analogues are yet to follow the function, specifically in terms of their stability and efficiency. This review discusses the rational design perspectives of both MOF and MOF-derived catalysts aiming to strengthen the prognostic ability toward the realization of the robust real-world electrocatalysts, capable of driving some of the most important electrochemical reactions of relevance for energy conversion, namely, HER, OER, CO_2RR, and the ORR (**Figure 1**). This review is not intended to be exhaustive and thus only presents an abridged account of some important works in line with the proposition. The reader is guided to some excellent reviews for a detailed understanding of the fundamentals of the different electrocatalytic reactions[17–19] discussed in this review.

In the frame of building a hydrogen economy, the splitting of water into molecular hydrogen and oxygen is the most viable option for producing a clean energy carrier gas for the large-scale implementation of fuel cell technology. The thermodynamically uphill oxygen evolution reaction involves a four-electron oxidation process of water molecules and is considered to be the bottleneck of the overall water-splitting ($2H_2O \rightarrow 2H_2 + O_2$; $\Delta E^\circ = 1.23$ V) reaction. The heterogeneous nature of these electrocatalytic reactions imposes the need to provide specific active sites for the adsorption of the reactants, followed by their multiple intermediate step transformation to finally facilitate the desorption of the products from the surface. Considering the variations in the physical, chemical, and electronic properties of the reactants, the adsorption energies involved in each of these steps are very much different from one another.[20] Therefore, the design of an active site demands a careful consideration of the interaction energies, strain, and steric effects involved in each of these intermediate steps. Importantly, as every electrocatalytic process demands the coexistence of rapid charge transfer across the extended reaction interface, it is also imperative to utilize design principles that lead to electrically conductive MOFs with high surface area, substantial porosity and good charge mobility, simultaneously.[21] The MOFs can be perceived as intrinsically highly ordered solid-state molecular metal sites, wherein functional motifs can be assembled into an array of a functionally repeating matrix. However, despite containing the active molecular structure, the poor charge transport properties of many chemically stable MOFs often restrain their effectiveness as direct electrocatalysts. Interestingly, owing to the occurrence of metal and organic species in its framework, MOFs are popular as self-sacrificial precursors or templates for deriving porous carbon-based composite materials with highly dispersed inorganic nanophases as catalytic active sites in combination with a porous network for enhanced mass transport. MOFs are typically heat-transformed into a conductive carbon-based composite matrix wherein the functional active sites are not only preserved but also firmly embedded inside the MOF templated skeleton.[22] The ligands of such MOFs usually contain heteroatoms (like N, S, and P) to tailor the electron donating or accepting properties of the resulting carbon composite.[9,23] It is undisputable that the

Harshitha Barike Aiyappa obtained her Ph.D. from the CSIR-National Chemical Laboratory, Pune, India in 2017. Her primary research interest focuses on the design and development of porous polymeric materials for electrocatalytic applications. She is currently an Alexander von Humboldt postdoctoral researcher in the group of Prof. Wolfgang Schuhmann, Department for Analytical Chemistry and Center for Electrochemical Sciences (CES), Ruhr-University Bochum.

Wolfgang Schuhmann studied chemistry at the University of Karlsruhe, and completed his Ph.D. with F. Korte in 1986 at the Technical University of Munich. After finishing his habilitation at Technical University of Munich in 1993, he was appointed professor for Analytical Chemistry at the Ruhr-University Bochum in 1996. His research interests cover a broad spectrum of different fields of electrochemistry, including micro- and nanoelectrochemistry, scanning electrochemical microscopy, biosensors, biofuel cells, development of electrocatalysts for energy conversion, batteries, photoelectrochemistry, electrochemical deposition of catalyst nanoparticles, and noble-metal free electrocatalysts among others.

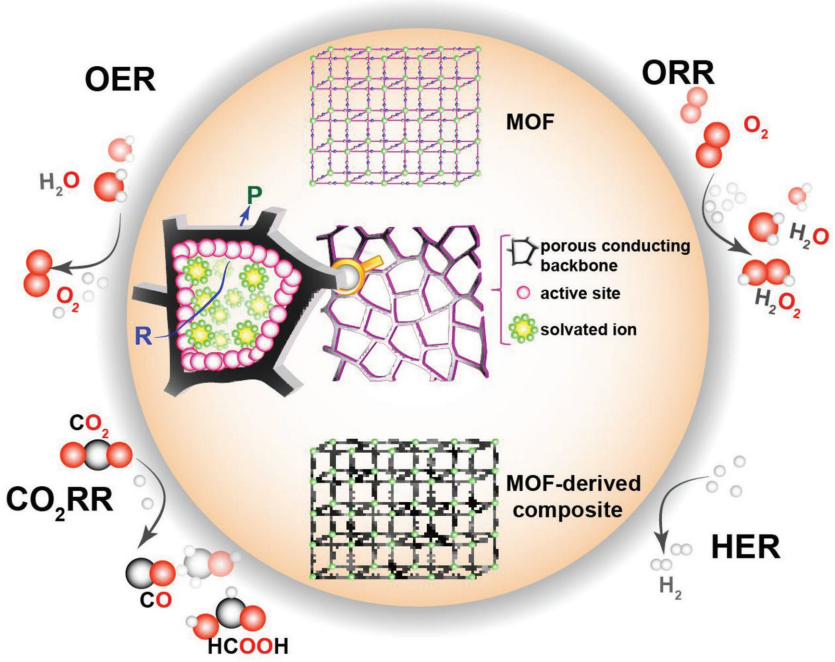

Figure 1. Potential electrocatalytic reactions driven by MOF/MOF-derived electrocatalysts.

physical and the chemical properties of the resulting "carbon composite" depend on the nature of the MOF precursor and the conditions used to derive it. Therefore, in order to achieve a targeted MOF or an MOF-derived electrocatalytic function, it is important to diligently select the metal and the ligand species, which can potentially offer active sites capable of driving the desired electrocatalytic reaction. The selection of active sites is generally influenced by (i) natural biological structures, which are mimicked to emulate their structure–property relations, (ii) mechanistic studies of the high energy intermediates of the reaction, (iii) inorganic species that are part of the active sites in the molecular catalysts, and (iv) computational activity–composition–structure predictions.

1.1. Guided by the Nature-Inspired Structural Motifs

Biological metalloproteins such as myoglobin (Mb) and hemoglobin (Hb) involve metal ions as cofactors to support their function. The intricate functioning of these structures with high selectivity and efficiency has intrigued an understanding of their structure–activity correlations. In particular, the role of the metal ions in promoting the chemical function of each metalloprotein is one of the principal interests of material science research. In general, many biological systems involve copper and iron-based active centers because of their ubiquitous occurrence in nature.[24] However, it is often observed that these metal ions do only function efficiently in the presence of certain coordinating ligands, which underscores the importance of the local environment on reactivity. Therefore, mimicking the structural configuration of such metallocomplexes necessitates a need to involve a dynamic metal–organic hybrid that can accommodate the concerted electron/proton transfer reactions occurring during the course of the reaction under consideration. The existence of metal ion-ligand coordination in its framework has popularized MOFs as a platform for emulating the structural features identical to the ones found in the metalloproteins. A rational design criterion principally involves translating the biological structural factors in MOFs by engaging the active metal ions in similar organic environments.[25] For instance, the cooperative insertion of CO_2 in the Mn—N bonds of a diamine-appended Mg-based MOF [mmen-Mg_2 (dobpdc)] to mimic the enzymatic pockets of Rubisco, a metallozyme involved in biological nitrogen fixation process.[26]

1.2. Guided by the Theoretical Understanding of the Reaction Mechanism

The Sabatier principle is one of the archetypal rules in catalysis. It asserts that the transformational ability of any catalytic surface depends on the binding energy of the intermediates formed during the course of the reaction. In accordance with Sabatier's principle, an ideal catalyst facilitates the binding of the key intermediate such that it is not only strong enough to attract the reactants to adsorb and react, but also weak enough to assist the easy desorption of the product formed.[27] Interestingly, volcano relations that typically arise from activity—adsorption descriptor plots often display discrepancies, owing to possible multiplicity of the active sites within the catalyst structures.[28,29] For instance, in the case of pyrolyzed MOFs, the active catalyst may comprise of metal centers coordinated to nitrogen (MN_x), nitrogen-functionalized carbon groups (CN_x) as well as metal oxide (MO_x) species, each of which possesses some inherent catalytic activity.[30] Most importantly, the theoretically derived "volcano plots" fail to include the influence of the local pH value, the presence of counter ions in the reaction medium and the impact of the position of the d-band center in the metal complex on the rate of an electrochemical reaction.[31,32] Moreover, these relations are only valid for catalytic surfaces that exhibit a similar reaction mechanism. So, despite being a sound approach, these plots cannot be the ultimate criterion for selecting the optimal catalysts for all kinds of reactions, owing to the complexity of the underlying factors and reaction dynamics in heterogeneous catalysis. Nevertheless, an understanding of the reactivity of the key intermediates and the activity of the catalyst material for a particular reaction is still crucial to "kick-start" the selection procedure. Thus, volcano plots can be observed as a useful guide to select suitable metal centers while designing a new catalyst structure.

1.3. Guided by Synthetic "Molecular Electrocatalysts"

Molecular electrocatalysts have been regularly employed as models to probe structure–property relations, given their

distinct advantage of forming reaction intermediates that can be isolated to elucidate the catalytic mechanisms. However, they suffer from a low density of catalytic sites, limited stability, and poor recyclability, wherein their heterogeneous counterparts excel. MOFs are considered as a bridging link between inorganic and polymeric functional materials. In order to design an electroactive MOF, the basic challenge is to identify such functional molecular units that can be possibly self-assembled to result into long-range ordered structures without losing their imprinted functionality.[14] It is important to keep in mind that during electrocatalysis, MOF structures may undergo activation transformation to produce catalytically active forms. For example, during OER electrocatalysis by a Co-ZIF-9(III), it was observed that the Co ion undergoes surface oxidation to cobalt oxyhydroxide prior to oxygen evolution, however, without affecting the bulk structure of the MOF.[33] Thus, it is imperative to design the frameworks such that they do not undergo any irreversible chemical alterations in the presence of the reactive adsorbates or the reaction conditions, which could otherwise challenge the structural integrity of the MOFs porous architecture.

1.4. Guided by Computational Activity–Composition–Structure Predictions

Understanding of the chemical changes at the surface occurring during the catalytic transformation is important in order to design an effective catalytically active surface. Molecular simulation techniques, in particular, quantum mechanical model-based density functional theory methods are regularly employed to theoretically describe (electrochemical) reactions at catalyst surfaces with great detail and high accuracy.[34] This method rationally simulates the variations in the catalytic activity arising from the differences in the material composition or structure and could therefore be used to design surfaces with predetermined catalytic activity.[35] Recent advances in simulation techniques have proposed numerous general relations that are believed to help understand trends in catalytic activity. For instance, the d-band centre is found critical for the bonding of adsorbates on transition metal surfaces.[36] It is observed that a linear relationship between the energy of activation and the enthalpy change of an elementary reaction step (i.e., the Brønsted–Evans–Polanyi relationship) is often followed.[37] Furthermore, a quantitative approach was also reported by evaluating the trends between the selectivity and the bond strength.[38] Thus, in combination with the practical assessments, computationally driven design principles also hold great promise in guiding the discovery of new catalytic surfaces.

2. Directed Engineering of a "Pristine" MOF Electrocatalyst

2.1. Toward OER

To date, molecular catalysts with structural resemblance to the active center of photosystem II and metal oxides are the two important variants of successfully tested "synthetic" water oxidation catalysts.[39] The formation of the O—O bond is supposed to result from the nucleophilic attack of water molecules at the high oxidation sites of the catalyst or via interaction of two adjacent M–O units within the catalytic structure.[17] In either of the case, a typical OER active surface should provide sites for accommodating the proton coupled electron transfer phenomenon (**Figure 2**a,b). Among the economical alternatives, the 3d transition metal oxide systems are found to exhibit OER activity comparable to that of the standard Ir/Ru-based precious OER catalysts. Using the OH_{ad}–$M^{2+\delta}$ interaction for OH^- as the primary descriptor, the reaction trends toward the OER are observed to follow the order Ni > Co > Fe > Mn.[40] From a material design standpoint, MOFs could be used as scaffolds to host such reducible oxide centers so that the O—O bond formation is entropically favored. Additionally, kinetically inert ligands could be chosen so that it does not degrade during the water oxidation reaction. Successful reports exist of OER activity in MOFs constructed using the above metal combinations. An enlightening example is a Ni- and Fe-based bimetallic MOF (with Fe/Ni atomic ratio = 23%) grown on a flexible 3D macroscopic nickel foam.[41] The NiO_6 units inside the MOF structure are projected to undergo oxidation forming NiO_6/NiOOH species, which then promote the oxidation of hydroxide ions into molecular oxygen in alkaline conditions. The Fe impurity is assumed to introduce

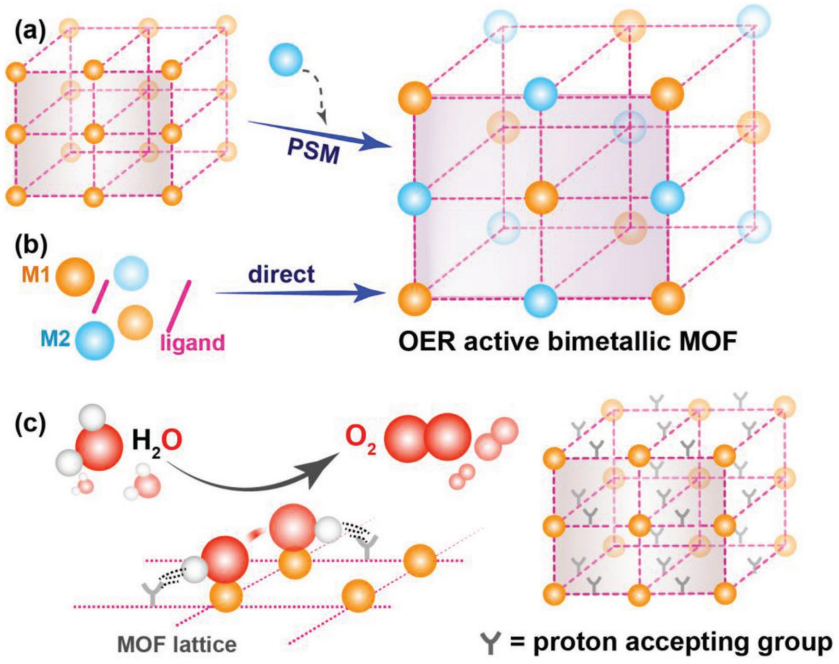

Figure 2. Strategies toward the development of the OER-active MOFs: Utilization of electroactive bimetallic ions in the MOF by a) postsynthetic modification or b) direct mixing. c) Illustration of the cooperative effect of the proton-accepting groups on the OER activity.

additional structural vacancies in the Ni-MOF structure thereby enhancing its catalytic activity. Furthermore, combinations of metal ions have proven successful in improving the electrocatalytic activity of some Co-based MOF nanosheets. The introduction of Ni^{2+} ions into the coordinatively unsaturated sites of a Co^{2+}-based ultrathin framework is reported to instigate a partial electron transfer from Ni^{2+} (with fully occupied t_{2g} d-orbitals) to high spin Co^{2+} site (with unpaired t_{2g} d-electrons) through the oxygen of the ligands.[42] This electronic coupling effect is observed to boost the π electron (ε^-) donation through the Co^{2+} centers, thereby improving the overall OER activity. In addition to the reactivity of the metal ions, the presence of coordinatively unsaturated metal sites may also boost the OER activity in MOFs. One of the interesting defect-based approaches is based on the atomic dispersion of the active sites in Co-based ZIF-67 by the partial removal of the coordinating ligands by means of plasma etching effects.[43] The high density of the unsaturated metal sites is believed to improve the interaction of the active sites with oxygen, thereby facilitating faster OER kinetics on the etched ZIF-67 surface. Remarkably, the constituting ligands are also expected to influence electronic perturbations of the redox centers in electroactive MOFs. During the OER, "protophilic" ligands are believed to act as a "local proton sink" and assist the deprotonation of the water molecules thereby facilitating the "O—O" bond formation (Figure 2c). In one such explicit display of ligand-assisted OER activity, the benzimidazolate motifs in the vicinity of the Co (II) centers in Co-ZIF-9 are observed to accept a proton and help in the initial dehydrogenation step of the water molecule.[33,44] MOFs with flexible ligand linkers can be expected to easily adapt to the electronic demands of the high oxidation states of the metal centers. In particular, the ligands with electron-withdrawing ability could be potentially employed to support the formation of reactive high oxidation state of metals. Thus, it can be concluded that an MOF with metal ions that can exhibit high oxidation states and ligands that are kinetically robust to evade self-oxidation could be productively used for catalyzing the OER.

2.2. Toward HER

Hydrogenases and nitrogenases contain Ni–Fe and Fe–Mo active sites for reversibly catalyzing the HER under aerobic conditions. The Ni atoms are largely accepted water dissociation centers, while the Mo atoms possess superior hydrogen adsorption properties. In addition, the presence of strong π–acceptor ligands such as CO and CN^- close to [Ni–Fe] active sites promotes the formation of low-spin Ni(III/II/I) oxidation states, which serve as active site for the HER.[45] Thus, it can be perceived that a surface which can promote the dissociation of water molecules besides supporting the hydrogen recombination step can be explored for catalyzing the HER (**Figure 3**a).

Important illustrations of nature's brilliant masterstroke are the Mo- and W-containing molybdopterin proteins, which are known to exhibit reversible redox behavior and high resistance to hydrogenation. The metal–dithiolene complexes are thereby one of the potential structural motifs that are explored for proton reduction reactions.[46] Using the MOF extended framework these units could be replicated yet well separated to minimize the chances of their deactivation via aggregation (Figure 3b). An example of this strategy is a report of the integration of the cobalt dithiolene complexes into a MOF.[47] The extended 2D supramolecular polymers show an improved exposure of catalytic sites, enhanced stability, improved adhesion to the surface alongside with maintaining the activity and reduction potential as that of their molecular analogues. Among the HER molecular catalysts, polyoxometallates (POMs) contain polyanionic molecular oxo-clusters of early transition metal ions in their highest oxidation state (W^{VI}, Mo^{VI}, or V^V), which can support reversible multivalence reduction/oxidation (Figure 3c).[48] In an explicit attempt to incorporate these soluble functional units into an MOF, the redox active $\{\varepsilon\text{-}PMo^{V}_{8}Mo^{VI}_{4}O_{36}(OH)_4\ Zn_4\}$ Keggin units modified with 1,3,5-benzene tricarboxylate linkers are capped by Zn(II) ions to result into a 3D electroactive POMOF.[49] Convincingly, the POMOFs are reported to display a pH-dependent electrocatalytic HER activity in aqueous medium. In an extension of this line of work, the ε-Keggin units are modified using benzene tribenzoate (resulting into NENU-500) and [1,1′-biphenyl]-3,4′,5-tricarboxylate linkers (resulting into NENU-501) to result in HER active POMOFs.[50]

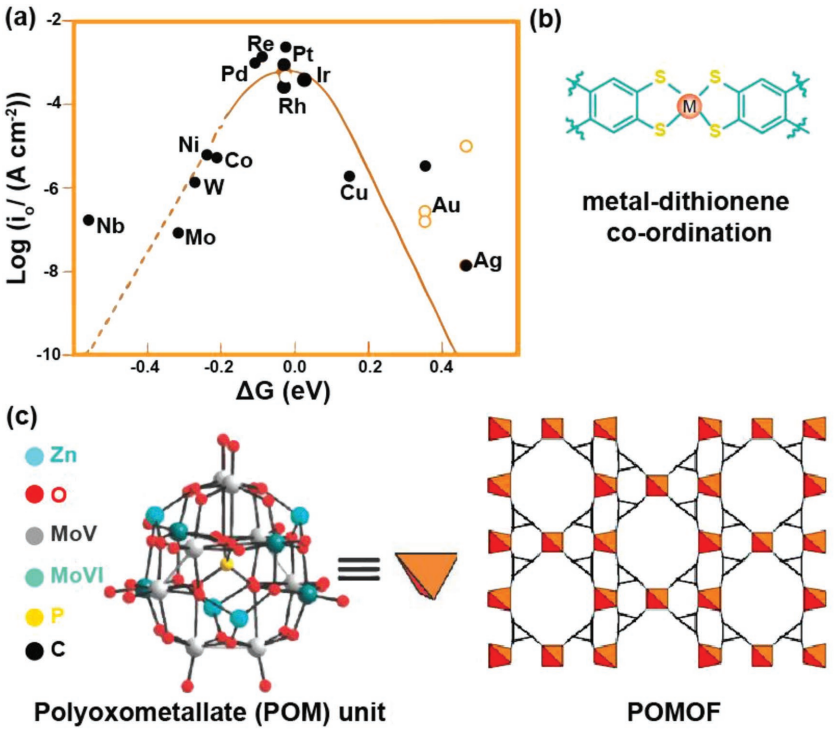

Figure 3. a) Volcano plots based on exchange current density versus the calculated free energy of H adsorption at $U = 0$ V. Adapted with permission.[102] Copyright 2010, American Chemical Society. b) Prospective metal–thionene coordination configuration used for the MOF synthesis. c) Ball-and-stick representation of the typical POM Keggin core and its incorporation in a ε $(trim)_{4/3}$ POMOF. Reproduced with permission.[49] Copyright 2011, American Chemical Society.

2.3. Toward CO_2RR

Electrochemical reduction of the kinetically inert and thermodynamically stable CO_2 molecule is an energy intensive process, often resulting in poor selectivity of the formed products. Metallated complexes involving macrocyclic ligands and polypyridine ligands are some of the coordination complexes that have been explored as homogeneous catalysts for the CO_2 reduction reaction (**Figure 4**a).[51,52] An extensive study reported using Fe(0) porphyrin systems underlines the synchronized actions of bimetallic sites for effective CO_2 reduction; an electron-rich center to initiate the CO_2 reduction and an electron-deficient Lewis acid site to complete the transformation.[53] One of the direct approaches used for introducing CO_2RR activity into MOFs is the integration of porphyrinic catalytic units into the MOF framework.[54] An important example is a report using chemically stable Fe-porphyrin containing Zr-based MOF-225 which contains electrochemically addressable catalytic site with a density of $\approx 10^{15}$ sites per cm^2.[55] The Fe centers in the porphyrin units of the framework exhibit a typical Fe(I/0) redox behavior, where CO_2 is reduced into CO. The active site of the fastest biological CO_2 sequestrating enzyme, carbonic anhydrase, contains a Zn^{2+}-based prosthetic group to initiate the hydration of CO_2. Interestingly, among the 3d transition metals, Zn is observed to display weak CO binding energy, which helps it evade the negative consequences of CO poisoning during the CO_2RR.[56] The propensity of the Zn^{2+} ions to reduce CO_2 is recorded in a robust ZIF-8 structure, wherein they undergo electroreduction into Zn^+ species, which are then catalytically active toward reducing CO_2 into CO.[57] Owing to their open framework structures, MOFs can be designed to specifically adsorb the reactant molecules via modulation of their metal ion–ligand junctions. In particular, MOFs containing open-metal sites and accessible coordination vacancies are observed to be potentially capable of accommodating electroactive guest molecules like CO_2 (Figure 4b).[58] Among the transition metal ions, Cu is estimated to possess moderate binding energy for CO, thereby offering a unique ability to reduce CO_2 to C_2 hydrocarbons with high selectivity and conversion efficiency.[59] This has prompted the exploration of numerous Cu-based MOFs as CO_2RR electrocatalysts. An initiative taken in this direction is a report using electrochemically synthesized Cu-HKUST, whose activity is tested after drop coating it onto a glassy carbon electrode surface.[60] It is proposed that the Lewis acid nature of the activated Cu(II) ions helps in stabilizing CO_2 via adduct formation, while its propensity to immediately reduce into Cu(I) catalyzes the CO_2RR to produce oxalic acid. Additionally, the porosity of the Cu-BTC framework is believed to act as a CO_2 reservoir in facilitating a concurrent sequestration as well as electroreduction within the pores. Apart from the reactive metal centers, in specific cases, the protogenic OH-based ligands are found to add-on the role of a local proton source and further boost the intrinsic activity of the MOF toward electrocatalytic reduction reactions like CO_2RR. In one such exemplary report, a dithiooxamide-based ligand is used to construct a Cu-based MOF.[61] The high selectivity of formic acid (over 98%) produced using CR-MOF electrode is proposed to be due to the presence of a proton source very close to the Cu(II) site. Protogenic ligands are believed to induce a local change in the proton concentration, subsequently decreasing the electron density at the metal ion centers. This in turn weakens the adsorption of CO_2 on the active site, resulting in the selective reduction of CO_2 into HCOOH.

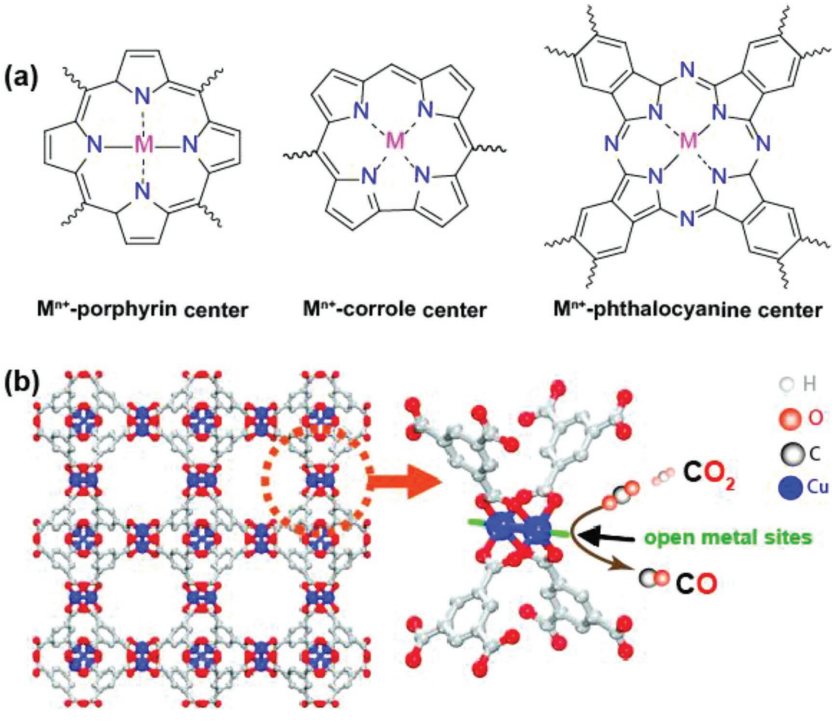

Figure 4. a) Macrocyclic ligands well-known to catalyze the CO_2RR. b) Illustrations of the HKUST-1 structure and the open metal coordination site in the Cu-paddlewheel environment. Reproduced with permission.[103] Copyright 2011, American Chemical Society.

2.4. Toward ORR

The oxygen reduction reaction typically proceeds through concerted proton–electron transfer pathways with the complete reduction ($4e^- + 4H^+$) of O_2 producing H_2O and the partial reduction ($2e^- + 2H^+$) pathway generating H_2O_2. The four electron transfer mechanism is the most energy rewarding conversion and therefore the desired reaction for energy applications.[7] In particular, the rate of the electrochemical cathodic ORR determines the ultimate performance of the fuel cells. A number of molecular models, mostly inspired by biological systems like hemoglobin (Hb), myoglobin (Mb), mitochondrial cytochrome c oxidase, etc. are developed to understand the steps influencing the kinetics and selectivity of the ORR.[62] Interestingly, each of these natural ORR sites is observed to perform specific functions;

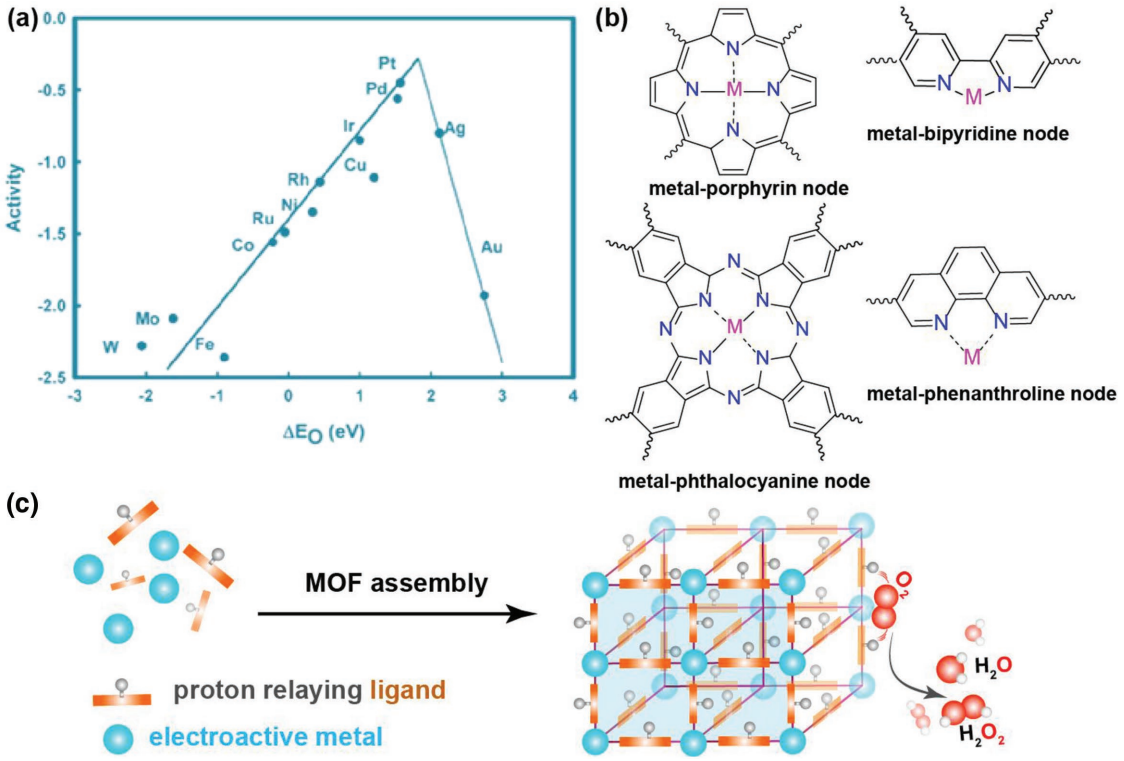

Figure 5. a) Volcano plot indicating the variations in the oxygen reduction activity as a function of the oxygen binding energy. Reproduced with permission.[104] Copyright 2004, American Chemical Society. b) Metal–ligand combinations for developing ORR-active MOFs. c) Illustration of the cooperative effect of the proton relaying ligand on the ORR activity.

Hb and Mb are only involved in reversible O_2 binding, while the cytochrome c oxidase is capable of reducing O_2 to H_2O. The studies underpin the role of the nature of the metal and ligands present in the catalytic structure in modulating the kinetics and selectivity of the ORR. For instance, laccase in the aerobic respiratory chains consists of a multicopper active core with catalytic activity reportedly outperforming the standard Pt catalysts.[63] The cytochrome c oxidase metalloprotein involves a binuclear heme and copper site that is responsible for the binding and subsequent reduction of molecular oxygen.[64] "M–N_4" coordination centers of these enzymes are the typically targeted structural motifs for ORR catalysts (**Figure 5**b). The possibilities of numerous metal–ligand coordinations in MOFs make them promising candidates for designing heterogeneous ORR catalysts. The first step of the ORR in alkaline electrolytes (toward producing both H_2O or H_2O_2) involves the transfer of an electron to O_2 to form superoxide ($O_2^{\bullet-}$), which in case of the metallated systems is typically coordinated to a metal center.[7] The oxygen adsorption strength (ΔG_{O*}) is the generally used catalytic descriptor representing the bond strength between the surface and the reaction intermediates (O*, OOH*, and OH*) (Figure 5a).[65] MOFs constructed using transition metal centers (typically Fe and Co) are observed to efficiently catalyze the ORR. Early reports of the intrinsic ORR activity in MOFs reported a water-stable Cu-bipy-BTC MOF, with the "Cu–N" groups expected to be the electroactive sites in a 0.1 M phosphate buffer (pH 6.0) solution.[66] The MOF exhibited a redox type catalysis involving the Cu (II/I) redox couple and pronounced ORR activity to produce water was observed. In another report, the ORR-active Fe-porphyrin units are embedded within a robust Zr-based MOF, $[Zr_6O_4(OH)_4(Fe(III)\text{-}(TCPP)_3)]$.[67] The redox-active Fe-porphyrin units are observed to catalyze ORR through the $4e^-$ pathway in 0.1 M $LiClO_4$/DMF. The employment of proton relaying moieties has been a major directive used to promote the transfer of the protons across the ORR-active centers (Figure 5c).[68] The intrinsic electrocatalytic ability of the MOFs is also found to largely depend on the redox activity and the pK_a of the comprising organic struts. One such observation is made using an electrically conductive HITP (2,3,6,7,10,11-hexaiminotriphenylene)-based Ni-MOF, $Ni_3(HITP)_2$.[69] Contrary to the usual observation, it is proposed that herein the Ni sites only contribute to the electronic structure of the active species but do not directly participate in the ORR activity. Rather, electrochemical and spectroscopic studies in conjunction with computational studies suggest that the redox activity of the organic ligand induces ORR activity in the system. The HITP ligand is found to efficiently mediate charge delocalization across the framework rendering the key intermediates accessible throughout the reaction. Likewise, the ligands could also be designed to impart stability to the constituting framework. For example, the electron withdrawing effect of the tetrapyrrole moiety is found to stabilize the Co (II) active centers in a 3D porphyrinic MOF.[70] It is perceived that separation of the unsaturated metal centers by the ligands increases the longevity of the catalytic activity in these extended structures.

3. Directed Designing of MOF-Derived Electrocatalysts

A large proportion of the state-of-the-art MOFs employed as electrocatalysts suffer from acute stability issues in both low and high pH aqueous electrolytes. The metal–ligand coordination often succumbs to hydrolysis in the presence of the reactant adsorbates, such as water, thereby impairing the direct use of virgin MOFs as electrocatalysts. In addition, the nature of the hard M^{n+}–redox inactive ligand coordination further renders poor electronic conductivity to the long-range architecture. Thus, attempts have been made to transform metal and heteroatom emblazoned MOFs into functional carbon-based composites, which can conveniently circumvent the conductivity and stability issues faced by its predecessors. Owing to the existence of metal and carbonaceous ligand junctions in its framework, MOFs can be readily employed as a self-sacrificial template for deriving functional carbon composites.[71] However, it is important to carefully choose the annealing conditions, as the properties of the final carbon composite heavily rely on its course of thermal activation.[72] It is important to observe that although this approach does not help in conserving the molecular structure of the MOF, the active metal coordination centers are largely retained. This approach is particularly important toward utilizing a large number of MOFs with significant metal–ligand combinations, that are either not chemically stable or suffer from poor conductivity issues.

3.1. Toward OER

The naturally occurring oxygen-evolving center in photosystem II (PSII) of the green plants comprises of a high oxidation state Mn_4CaO_x "cubane" cluster.[73] Thus, functional motifs like spinel oxides with structural resemblance to the "cubane" structure are typically explored for catalyzing water oxidation reactions (**Figure 6**). The possibility of designing MOFs with multiple metal ions presents the opportunity to integrate such centers in the MOF backbone. In addition to providing large extended reaction interfaces, MOFs could be viewed as effective snares that prevent the agglomeration of active metal oxide particles, which could otherwise diminish the density of accessible active sites and their utilization. In this context, MOF structures could be viewed as simple yet versatile precursors for deriving OER active phases. For instance, a bimetallic $Mn_3[Co(CN)_6]_2$ Prussian blue analogous MOF consisting of a high oxidation state Co(+2.46) and Mn(+2.69) was used to derive "cubane" bearing spinel cobalt manganese oxide nanocubes to drive the OER in 0.1 M NaOH.[74] In another instance, a series of Fe and Ni-based MOFs are oxidatively transformed into Fe_xNi_x –oxides, predominantly with spinel $NiFe_2O_4$ structure, which display composition-dependent OER activity in 0.1 M KOH.[75] Likewise, the thermal synthesis of $M_xCo_{3-x}O_4$ (M = Co, Mn, Fe) porous nanocage materials was reported by precisely controlling the composition of metals in Prussian blue analogues, $M_3[Co(CN)_6]_2$ (M = Co, Mn, Fe).[76] Further, on-site mild oxidation of metal centers into atomically dispersed metal oxide species is also perceived to induce OER activity in MOF-derived structures. For instance, O_2 plasma treatment of ZIF-67 is observed to produce atomic-scale CoO_x species, which are capable of catalyzing OER with activity superior to the standard RuO_2 electrocatalyst at alkaline pH conditions.[77]

3.2. Toward HER

The HER is a typical two-electron transfer reaction whose rate is largely determined by ΔG_H, the hydrogen adsorption free energy. Thus, it is expected that the metals which can optimally bind hydrogen, also referred as "overpotential-deposited hydrogen" (H_{ad}), should display the highest catalytic activity.[78] However, as the volcano plots which reflect Sabatier's principle do not include the (local) pH effects, violations in the activity trend at different pH conditions are usually observed.[31] Moreover, it is important to understand that as water is a potential hydrogen donor in alkaline media, the catalyst surface should not have any strong affinity to adsorb the spectator hydroxide ions, which could otherwise passivate the catalyst.[79] An important investigation of the HER activity on Pt electrodes modified with 3D transition metal systems highlights the stability of 3d-$TM(OH)_2$ clusters (mainly Ni, Co, Fe, and Mn) in the potential range of interest.[40] A metal coordination center with optimum hydrogen interaction energy and water dissociating ability could be primarily considered for catalyzing the HER. In addition to metal oxides, corresponding sulfide/selenide/phosphide centers are also known to promote HER activity in both acidic and basic environments.[80,81] In order to ensure

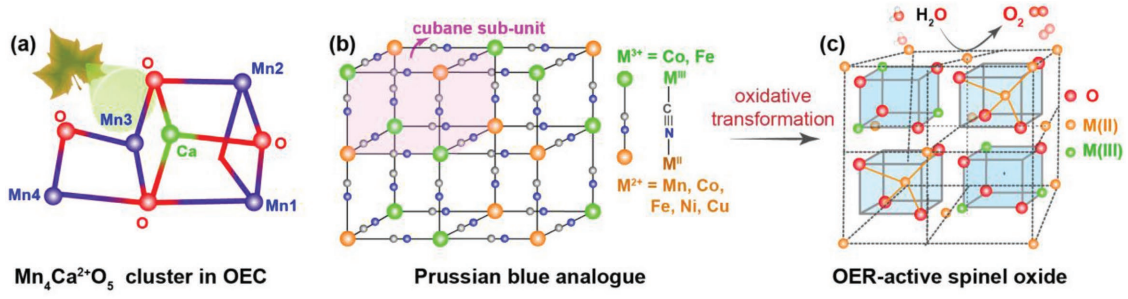

Figure 6. Nature-inspired design of OER-active MOF-derived materials. a) Illustration of $Mn_4Ca^{2+}O_5$ cluster of PS-II. Adapted with permission.[105] Copyright 2017, Macmillan Publishers Limited, part of Springer Nature. b) Illustration of the "cubane" units in Prussian blue analogues structures and c) illustration of spinel oxide structures obtained after their oxidative transformation.

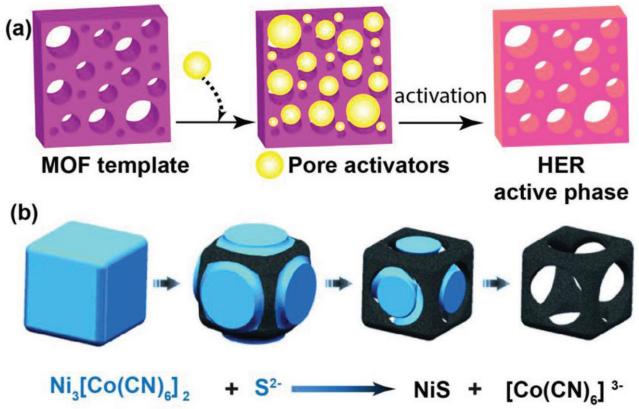

Figure 7. a) Inducing the HER activity in MOFs after post-synthetic modification. b) Exemplary representation of the formation of NiS nanoframes using a Ni–Co Prussian blue analogous MOF. Reproduced with permission.[82] Copyright 2015, Wiley-VCH.

porosity in the forming structures Co, Ni, Mo-based porous MOFs were used as precursors for generating such HER-active phases (**Figure 7**a). In most of the cases, the annealed MOFs are often subjected to sulfurization/phosphorization/selenization to produce M–S, M–P, and M–Se coordination centers. For example, nanocubes of Ni–Co Prussian blue analogues are observed to structurally transform into HER-active NiS hollow structures when treated with Na_2S under annealing conditions (Figure 7b).[82] In a typical strategy used to effectively disperse the HER-active sites, a bimetallic MOF is used to derive Ni–Co mixed metal phosphide nanotubes via two solid-state reaction steps.[83] The Co_4Ni_1P nanotubes possess similar morphology to their parent MOF precursor and show remarkable HER performance in 1 M KOH. Likewise, selenization of a Ni- and Fe-based bimetallic MOF results in $NiSe_2/Fe_3Se_4$/C hybrids, which are found to be active toward catalyzing the HER in alkaline conditions.[84]

3.3. Toward CO_2RR

Anaerobic bacteria contain $NiFe_4S_4$-centered carbon monoxide dehydrogenases (CODHs) that are known to efficiently reversibly catalyze the reduction of CO_2 to CO at room temperature.[85] During the catalysis CO_2 initially bridges to both Ni and Fe sites. The Lewis basicity of the Ni center helps in the electron transfer to the antibonding lowest unoccupied molecular orbital of CO_2 (**Figure 8**a). The resulting increase in the negative partial charges at the oxygen atoms is sequentially stabilized by the Lewis-acidic Fe center and the hydrogen bonds of the amino acid residues within the metalloenzyme. These biological models suggest that an "amphoteric" structure with similar electron rich and electron deficient nuclear configurations can be explored for generating a CO_2RR active material. Interestingly, heteroatom-doped carbons are the recent class of metal-free substrates identified to exhibit CO_2 reducing characteristics.[86,87] In particular, the CO_2RR activity is believed to originate from the interaction between the acidic CO_2 and Lewis basic pyridinic carbon groups present in nitrogen-doped carbon structures.[88] In this direction, MOFs could be explored as precursors for synthesizing porous nitrogen-doped carbon structures, preferably with pyridinic N defects, which are known to potentially form adducts with CO_2 molecules.[89] A seminal work in this direction used N-doped carbon derived by thermal treatment of a Zn-based ZIF-8.[23] The electron rich pyridinic-N and electron deficient quaternary-N groups in the porous carbon are proposed to synergistically stabilize the COOH* intermediate, thereby imparting catalytic activity to the carbon structure. Interestingly, in the case of ZIF-derived carbon composites, the presence of low coordinated M–N_x sites is observed to favor the stabilization of the anion radical formation during the CO_2 reduction reaction (Figure 8b,c).[90] Such active sites are usually created by involving bimetallic MOFs with Zn^{2+} as one of the ions. The reduced Zn evaporates during carbonization leaving atomically dispersed Co atoms behind, which are thereafter anchored on a N-doped porous carbon matrix.

3.4. Toward ORR

The use of metallated macrocycles as fuel cell cathode catalysts has gained momentum ever since Jasinski initially investigated the ORR activity of M–phthalocyanine (M = Co, Ni, Pt, Cu) complexes in alkaline medium.[91] The highly delocalized π-electron cloud in the macrocyclic ring is believed to activate fast reaction kinetics in such complexes. Following this finding, a wide spectrum of organometallic compounds based on structurally

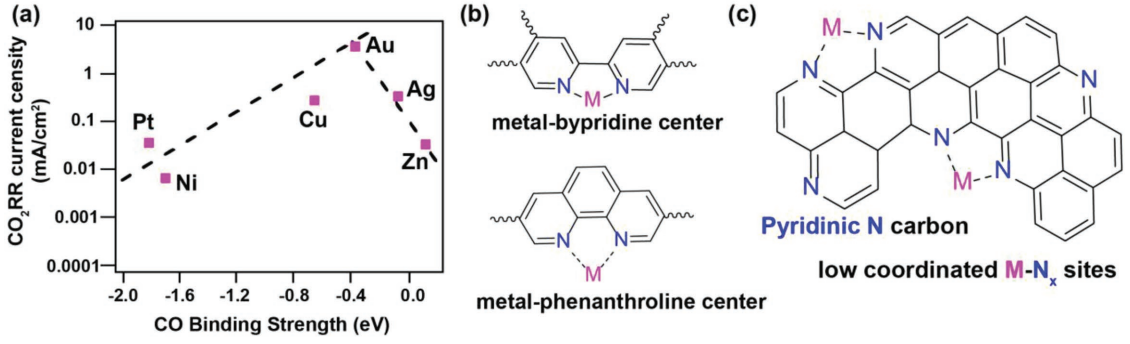

Figure 8. a) Volcano plot for CO_2 reduction activity as a function of the CO binding strength. Adapted with permission.[56] Copyright 2014, American Chemical Society. b) Metal–ligand coordinations useful as CO_2RR active sites. c) Illustration of desired heteroatom carbon structures for the CO_2RR.

related porphyrins or phenanthroline complexes have been tried for catalyzing the ORR.[7] The (M–N_x) motif of this catalytic system is often used as reference architecture for the molecular design of synthetic ORR electrocatalysts.[92] A large number of soluble molecular catalysts containing such structural motifs have successfully yielded ORR activity. However, the slow diffusion and poor mass transport within the thick electrocatalyst films often limits their activity. A mechanistic insight into the functioning of the biological metalloproteins underlines a golden rule that in order to attain a high rate of electron transfer, the redox sites should not be separated by a distance of more than 15 Å.[93] One way of effectively harnessing the utility of such systems is the direct immobilization of catalytic thin films on the electrode surface. However, in such a case, the increased proximity of the catalytic sites could not only aggravate the deleterious effects of catalyst aggregation butalso restrict the active site density due to limited film thickness. A more pragmatic move is to engage electron transfer mediators like carbon particles to relay electrons across the catalytic sites. In this direction, porous MOFs constructed using "M–N_x" coordination sites could be viewed as potential precursors for increasing the lifetime of such catalyticallyactive sites.[92] Crystalline MOF structures can be judiciously treated to produce chemically stable and porous M–N_x/carbon composites in which the structural motifs are conserved and effectively embedded within a conductive network.[22] One of the works in this direction is the use of a cobalt-imidazolate framework, which is observed to transform into an ORR active state following thermal treatment under an inert atmosphere.[94] During the activation, the metal ion centers of the parent ZIF are conserved while the rest of the imidazole linkers convert into a conductive N-doped carbon framework (**Figure 9**a). Structurally, the catalyst is assumed to possess the "Co–N_4" motif embedded within the N-doped carbon matrix. One of the smart strategies employed for precisely controlling the spatial dispersion and coordination structure in the MOF derived composite is the insertion of 'volatile' metal ions in the MOF lattice.[95] This approach is very well illustrated using a bimetallic ZIF structure.[96] Herein, the Zn^{2+} ions are strategically placed as spacers between the Co^{2+} sites in the ZIF lattice to prevent the Co sites from agglomerating during the thermal treatment (Figure 9b). On heating the Zn/Co ZIF, the Zn atom evaporate at ≈900 °C leaving the reduced and well separated Co single atoms in the N-doped porous carbon behind. The utilization of MOFs with transition metals that can induce graphitization of carbon is also observed to promote the stability of such MOF-derived composites. Furthermore, the annealing conditions can be adjusted to tune the reactivity of the catalyst structure.[97] In one such typical approach, Co-based ZIFs are treated under a reducing atmosphere (He containing traces of H_2) to induce the formation of Co/CoC_x/CoN_x structures encapsulated within a graphitic carbon matrix.[30,98] The embedded "Co–N_x" moieties and N-functionalized groups in the carbon framework are proposed to impart ORR activity to such MOF-derived composites. In order to induce the creation of OER active "Co–O" sites, the resulting composite is further subjected to controlled

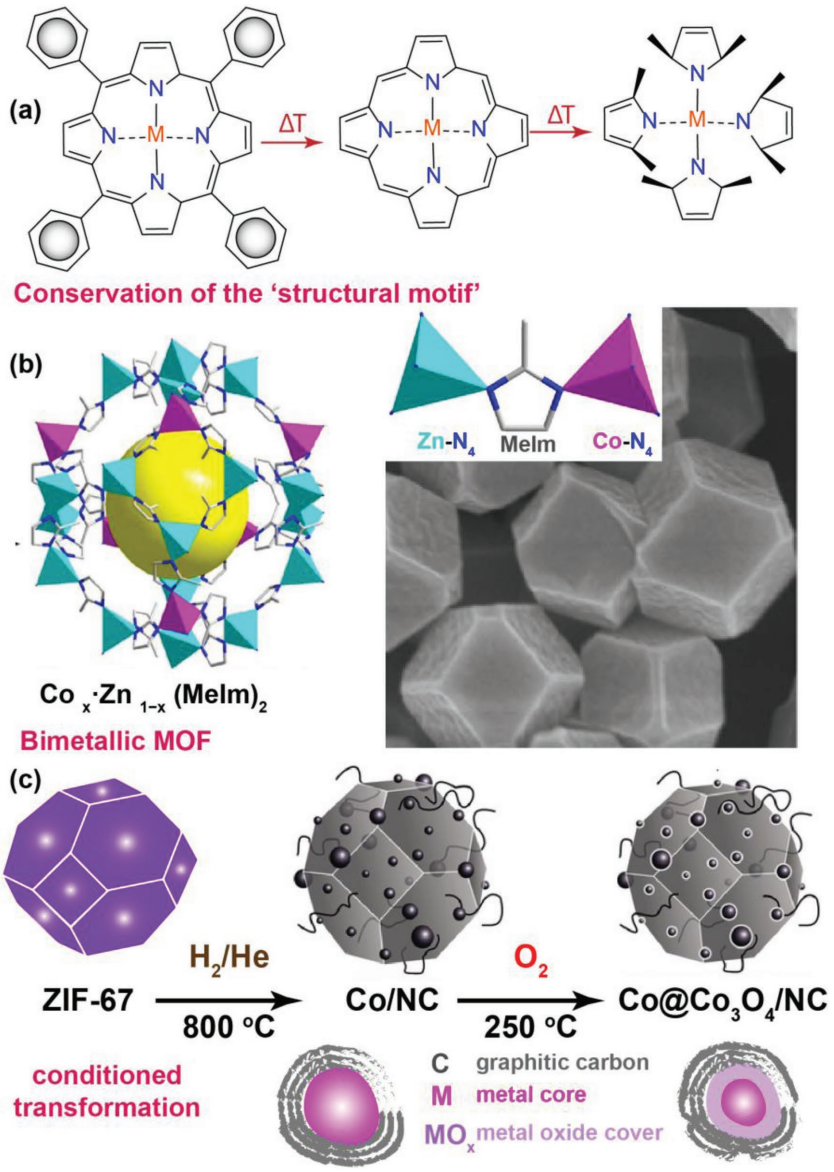

Figure 9. a) Conceptual illustration of the retention of metal coordination during heat treatment. Adapted with permission.[22] Copyright 2002, American Chemical Society. b) Crystal structure of a typical Co- and Zn-based bimetallic ZIF, and SEM image of one of the variants $Co_{0.1}Zn_{0.9}(MeIm)_2$. Reproduced under the terms of the CC BY 4.0 license.[95] Copyright 2016, Nature Publishing Group. c) Representation of the formation of core–shell nanoparticles via reductive carbonization of a typical ZIF-67 structure. Reproduced with permission.[30] Copyright 2016, Wiley-VCH.

mild calcination.[30] This treatment expedites the partial oxidation of the metallic cobalt surfaces resulting in the formation of core–shell spinel $Co@Co_3O_4$ nanoparticles encapsulated in a N-doped carbon nanotube-grafted carbon polyhedral matrix (Figure 9c). This treatment also facilitates the removal of the amorphous carbon covering the active metal centers, thereby increasing the electrocatalytic response of such MOF-derived composites. Additionally, the tuning of the metal composition of the MOF structure is also reported to improve the catalytic activity and stability of some of the MOF-derived carbon materials.[99] The effective utilization of the metal sites in such an MOF-derived matrix is further observed to improve by atomically dispersing the metal sites within the MOF-derived matrix. In one such report, a mixed-ligand strategy was used to achieve single atom Fe-implantation in a N-doped MOF-derived matrix.[100] Herein, a nonmetallated porphyrinic ligand was inserted to spatially separate the Fe-metallated porphyrinic ligand in the MOF matrix, which effectively suppresses the aggregation of the Fe centers during the subsequent pyrolysis of the MOF.

4. Conclusion and Outlook

The review outlines prospective approaches through which MOF-based materials can be rationally designed to achieve desired electrocatalytic properties. It illuminates the role of nature inspired biological structural factors, synthetic molecular catalysts, their thermally derived counterparts, and the need for solid understanding of the particularities of the electrocatalytic reaction in influencing the rational design of the targeted structure. Specifically, it can be outlined that designing of MOF-based electrocatalysts demands an in-depth understanding of the nature of the reaction intermediates formed and the configuration of the active sites needed to stabilize these transient species. Working toward this goal, it is important to judiciously choose suitable metal–ligand combinations apart from ensuring the provision of a high surface area reaction interface within the MOF architecture. Herein, the primary challenge is to identify the key structural motifs that govern the specific catalytic pathways and the ways in which they can be employed to reproduce the catalytic function in the MOF/MOF-derived matrix. In case of bioinspired structural motifs, the coordination environment should be highly regarded to obtain the desired structure–property relation. The chemical stability of the metal–ligand coordination under catalytic conditions must be additionally ensured for a stable performance. The spatial dispersion of the recognized active sites is also identified to significantly increase the utilization of the extended MOF surface. The potential combinations of metal ions, as indicated by the theoretical understanding of the reaction pathways, can be alongside implemented to tune the reactivity of the metal centers. Besides improving the competence of the metal nodes, the electronic perturbations of the constituting ligands is also observed to influence the activity of the MOF derived catalyst in terms of the reaction kinetics and catalytic turnover number. Furthermore, it is also perceived that the above-mentioned strategies can be very much extended to screen and design catalysts for broader electrocatalytic applications like, e.g., ammonia synthesis, methanol oxidation, hydroxymethylfurfural (HMF) oxidation reactions among others. For instance, Fe-based MOFs can be modified to emulate the 4Fe–4S clusters of the enzyme nitrogenase under formation of $Fe–S_x/Fe–P_x$ based active centers, which are proposed to catalyze the electroreduction of N_2 at room temperature.[101] It is therefore hoped that the review will inspire informed design and selection of MOFs in electrocatalysis and broaden their application beyond mere recognition as intriguing materials of laboratory curiosity.

Acknowledgements

The authors acknowledge financial support by the BMBF in the framework of the project "NEMEZU" (03SF0497B) and the Deutsche Forschungsgemeinschaft in the framework of the Cluster of Excellence "RESOLV" (EXC1069). H.B.A. acknowledges the Alexander von Humboldt foundation for a Postdoc fellowship.

Conflict of Interest

The authors declare no conflict of interest.

Keywords

electrocatalysis, energy conversion, metal–organic frameworks, MOF-derived catalysts

Received: October 16, 2018
Revised: November 1, 2018
Published online:

[1] M. Shao, Q. Chang, J.-P. Dodelet, R. Chenitz, *Chem. Rev.* **2016**, *116*, 3594.
[2] H.-F. Wang, C. Tang, Q. Zhang, *Adv. Funct. Mater.* **2018**, *488*, 1803329.
[3] Y. P. Zhu, C. Guo, Y. Zheng, S.-Z. Qiao, *Acc. Chem. Res.* **2017**, *50*, 915.
[4] C. Tang, H.-F. Wang, Q. Zhang, *Acc. Chem. Res.* **2018**, *51*, 881.
[5] J. Zhang, Z. Xia, L. Dai, *Sci. Adv.* **2015**, *1*, e1500564.
[6] Y. Zhang, Q. Zhou, J. Zhu, Q. Yan, S. X. Dou, W. Sun, *Adv. Funct. Mater.* **2017**, *27*, 1702317.
[7] M. L. Pegis, C. F. Wise, D. J. Martin, J. M. Mayer, *Chem. Rev.* **2018**, *118*, 2340.
[8] J. Wang, J. Wang, Z. Kong, K. Lv, C. Teng, Y. Zhu, *Adv. Mater.* **2017**, *29*, 1703044.
[9] L. Yang, X. Zeng, W. Wang, D. Cao, *Adv. Funct. Mater.* **2018**, *28*, 1704537.
[10] P.-Q. Liao, J.-Q. Shen, J.-P. Zhang, *Coord. Chem. Rev.* **2018**, *373*, 22.
[11] H. Zhang, X. Liu, Y. Wu, C. Guan, A. K. Cheetham, J. Wang, *Chem. Commun.* **2018**, *54*, 5268.
[12] Z. Liang, C. Qu, W. Guo, R. Zou, Q. Xu, *Adv. Mater.* **2018**, *30*, e1702891.
[13] H. Furukawa, K. E. Cordova, M. O'Keeffe, O. M. Yaghi, *Science* **2013**, *341*, 1230444.
[14] C. A. Downes, S. C. Marinescu, *ChemSusChem* **2017**, *10*, 4374.
[15] Y. Qian, I. A. Khan, D. Zhao, *Small* **2017**, *13*, 1701143.
[16] W. Tu, Y. Xu, S. Yin, R. Xu, *Adv. Mater.* **2018**, *30*, 1705106.

[17] X. Sala, S. Maji, R. Bofill, J. García-Antón, L. Escriche, A. Llobet, *Acc. Chem. Res.* **2014**, *47*, 504.
[18] L. Zhang, Z.-J. Zhao, J. Gong, *Angew. Chem., Int. Ed.* **2017**, *56*, 11326.
[19] Z. Liang, H. S. Ahn, A. J. Bard, *J. Am. Chem. Soc.* **2017**, *139*, 4854.
[20] V. R. Stamenkovic, D. Strmcnik, P. P. Lopes, N. M. Markovic, *Nat. Mater.* **2016**, *16*, 57.
[21] L. Sun, M. G. Campbell, M. Dincă, *Angew. Chem., Int. Ed.* **2016**, *55*, 3566.
[22] A. L. Bouwkamp-Wijnoltz, W. Visscher, J. A. R. van Veen, E. Boellaard, A. M. van der Kraan, S. C. Tang, *J. Phys. Chem. B* **2002**, *106*, 12993.
[23] R. Wang, X. Sun, S. Ould-Chikh, D. Osadchii, F. Bai, F. Kapteijn, J. Gascon, *ACS Appl. Mater. Interfaces* **2018**, *10*, 14751.
[24] E. Frieden, *Trends Biochem Sci.* **1976**, *1*, 273.
[25] C. H. Hendon, A. J. Rieth, M. D. Korzyński, M. Dincă, *ACS Cent. Sci.* **2017**, *3*, 554.
[26] T. M. McDonald, J. A. Mason, X. Kong, E. D. Bloch, D. Gygi, A. Dani, V. Crocellà, F. Giordanino, S. O. Odoh, W. S. Drisdell, B. Vlaisavljevich, A. L. Dzubak, R. Poloni, S. K. Schnell, N. Planas, K. Lee, T. Pascal, L. F. Wan, D. Prendergast, J. B. Neaton, B. Smit, J. B. Kortright, L. Gagliardi, S. Bordiga, J. A. Reimer, J. R. Long, *Nature* **2015**, *519*, 303.
[27] Z. W. Seh, J. Kibsgaard, C. F. Dickens, I. Chorkendorff, J. K. Nørskov, T. F. Jaramillo, *Science* **2017**, *355*, eaad4998.
[28] N. B. Halck, V. Petrykin, P. Krtil, J. Rossmeisl, *Phys. Chem. Chem. Phys.* **2014**, *16*, 13682.
[29] A. R. Zeradjanin, J.-P. Grote, G. Polymeros, K. J. J. Mayrhofer, *Electroanalysis* **2016**, *28*, 2256.
[30] A. Aijaz, J. Masa, C. Rösler, W. Xia, P. Weide, A. J. R. Botz, R. A. Fischer, W. Schuhmann, M. Muhler, *Angew. Chem., Int. Ed.* **2016**, *55*, 4087.
[31] P. Quaino, F. Juarez, E. Santos, W. Schmickler, *Beilstein J. Nanotechnol.* **2014**, *5*, 846.
[32] C. Costentin, J.-M. Savéant, *Nat. Rev. Chem.* **2017**, *1*, 87.
[33] K. Jayaramulu, J. Masa, D. M. Morales, O. Tomanec, V. Ranc, M. Petr, P. Wilde, Y.-T. Chen, R. Zboril, W. Schuhmann, R. A. Fischer, *Adv. Sci.* **2018**, *103*, 1801029.
[34] J. K. Nørskov, T. Bligaard, J. Rossmeisl, C. H. Christensen, *Nat. Chem.* **2009**, *1*, 37.
[35] C. Poree, F. Schoenebeck, *Acc. Chem. Res.* **2017**, *50*, 605.
[36] B. Hammer, J. K. Norskov, *Nature* **1995**, *376*, 238.
[37] R. A. van Santen, M. Neurock, S. G. Shetty, *Chem. Rev.* **2010**, *110*, 2005.
[38] F. Studt, F. Abild-Pedersen, T. Bligaard, R. Z. Sørensen, C. H. Christensen, J. K. Nørskov, *Science* **2008**, *320*, 1320.
[39] W. T. Hong, M. Risch, K. A. Stoerzinger, A. Grimaud, J. Suntivich, Y. Shao-Horn, *Energy Environ. Sci.* **2015**, *8*, 1404.
[40] R. Subbaraman, D. Tripkovic, K.-C. Chang, D. Strmcnik, A. P. Paulikas, P. Hirunsit, M. Chan, J. Greeley, V. Stamenkovic, N. M. Markovic, *Nat. Mater.* **2012**, *11*, 550.
[41] J. Duan, S. Chen, C. Zhao, *Nat. Commun.* **2017**, *8*, 15341.
[42] S. Zhao, Y. Wang, J. Dong, C.-T. He, H. Yin, P. An, K. Zhao, X. Zhang, C. Gao, L. Zhang, J. Lv, J. Wang, J. Zhang, A. M. Khattak, N. A. Khan, Z. Wei, J. Zhang, S. Liu, H. Zhao, Z. Tang, *Nat. Energy* **2016**, *1*, 404.
[43] L. Tao, C.-Y. Lin, S. Dou, S. Feng, D. Chen, D. Liu, J. Huo, Z. Xia, S. Wang, *Nano Energy* **2017**, *41*, 417.
[44] S. Wang, Y. Hou, S. Lin, X. Wang, *Nanoscale* **2014**, *6*, 9930.
[45] H. Ogata, W. Lubitz, Y. Higuchi, *J. Biochem.* **2016**, *160*, 251.
[46] W. R. McNamara, Z. Han, P. J. Alperin, W. W. Brennessel, P. L. Holland, R. Eisenberg, *J. Am. Chem. Soc.* **2011**, *133*, 15368.
[47] A. J. Clough, J. W. Yoo, M. H. Mecklenburg, S. C. Marinescu, *J. Am. Chem. Soc.* **2015**, *137*, 118.
[48] M. Sadakane, E. Steckhan, *Chem. Rev.* **1998**, *98*, 219.
[49] B. Nohra, H. El Moll, L. M. Rodriguez Albelo, P. Mialane, J. Marrot, C. Mellot-Draznieks, M. O'Keeffe, R. Ngo Biboum, J. Lemaire, B. Keita, L. Nadjo, A. Dolbecq, *J. Am. Chem. Soc.* **2011**, *133*, 13363.
[50] J.-S. Qin, D.-Y. Du, W. Guan, X.-J. Bo, Y.-F. Li, L.-P. Guo, Z.-M. Su, Y.-Y. Wang, Y.-Q. Lan, H.-C. Zhou, *J. Am. Chem. Soc.* **2015**, *137*, 7169.
[51] M. Bourrez, F. Molton, S. Chardon-Noblat, A. Deronzier, *Angew. Chem., Int. Ed.* **2011**, *50*, 9903.
[52] C. Costentin, M. Robert, *Acc. Chem. Res.* **2015**, *48*, 2996.
[53] M. Hammouche, D. Lexa, M. Momenteau, J. M. Saveant, *J. Am. Chem. Soc.* **1991**, *113*, 8455.
[54] N. Kornienko, Y. Zhao, C. S. Kley, C. Zhu, D. Kim, S. Lin, C. J. Chang, O. M. Yaghi, P. Yang, *J. Am. Chem. Soc.* **2015**, *137*, 14129.
[55] I. Hod, M. D. Sampson, P. Deria, C. P. Kubiak, O. K. Farha, J. T. Hupp, *ACS Catal.* **2015**, *5*, 6302.
[56] K. P. Kuhl, T. Hatsukade, E. R. Cave, D. N. Abram, J. Kibsgaard, T. F. Jaramillo, *J. Am. Chem. Soc.* **2014**, *136*, 14107.
[57] Y. Wang, P. Hou, Z. Wang, P. Kang, *ChemPhysChem* **2017**, *18*, 3142.
[58] J. Park, H. Kim, S. S. Han, Y. Jung, *J. Phys. Chem. Lett.* **2012**, *3*, 826.
[59] X. Liu, J. Xiao, H. Peng, X. Hong, K. Chan, J. K. Nørskov, *Nat. Commun.* **2017**, *8*, 15438.
[60] R. Senthil Kumar, S. Senthil Kumar, M. Anbu Kulandainathan, *Electrochem. Commun.* **2012**, *25*, 70.
[61] R. Hinogami, S. Yotsuhashi, M. Deguchi, Y. Zenitani, H. Hashiba, Y. Yamada, *ECS Electrochem. Lett.* **2012**, *1*, H17.
[62] J. A. Cracknell, K. A. Vincent, F. A. Armstrong, *Chem. Rev.* **2008**, *108*, 2439.
[63] M. S. Thorum, C. A. Anderson, J. J. Hatch, A. S. Campbell, N. M. Marshall, S. C. Zimmerman, Y. Lu, A. A. Gewirth, *J. Phys. Chem. Lett.* **2010**, *1*, 2251.
[64] S. Chatterjee, K. Sengupta, S. Hematian, K. D. Karlin, A. Dey, *J. Am. Chem. Soc.* **2015**, *137*, 12897.
[65] I. C. Man, H.-Y. Su, F. Calle-Vallejo, H. A. Hansen, J. I. Martínez, N. G. Inoglu, J. Kitchin, T. F. Jaramillo, J. K. Nørskov, J. Rossmeisl, *ChemCatChem* **2011**, *3*, 1159.
[66] J. Mao, L. Yang, P. Yu, X. Wei, L. Mao, *Electrochem. Commun.* **2012**, *19*, 29.
[67] P. M. Usov, B. Huffman, C. C. Epley, M. C. Kessinger, J. Zhu, W. A. Maza, A. J. Morris, *ACS Appl. Mater. Interfaces* **2017**, *9*, 33539.
[68] C. T. Carver, B. D. Matson, J. M. Mayer, *J. Am. Chem. Soc.* **2012**, *134*, 5444.
[69] E. M. Miner, S. Gul, N. D. Ricke, E. Pastor, J. Yano, V. K. Yachandra, T. van Voorhis, M. Dincă, *ACS Catal.* **2017**, *7*, 7726.
[70] M. Lions, J.-B. Tommasino, R. Chattot, B. Abeykoon, N. Guillou, T. Devic, A. Demessence, L. Cardenas, F. Maillard, A. Fateeva, *Chem. Commun.* **2017**, *53*, 6496.
[71] B. Liu, H. Shioyama, T. Akita, Q. Xu, *J. Am. Chem. Soc.* **2008**, *130*, 5390.
[72] H.-L. Jiang, B. Liu, Y.-Q. Lan, K. Kuratani, T. Akita, H. Shioyama, F. Zong, Q. Xu, *J. Am. Chem. Soc.* **2011**, *133*, 11854.
[73] C. Chen, J. Kazimir, G. M. Cheniae, *Biochemistry* **1995**, *34*, 13511.
[74] M. Abirami, S. M. Hwang, J. Yang, S. T. Senthilkumar, J. Kim, W.-S. Go, B. Senthilkumar, H.-K. Song, Y. Kim, *ACS Appl. Mater. Interfaces* **2016**, *8*, 32778.
[75] J. Jiang, C. Zhang, L. Ai, *Electrochim. Acta* **2016**, *208*, 17.
[76] J. Wei, Y. Feng, Y. Liu, Y. Ding, *J. Mater. Chem. A* **2015**, *3*, 22300.
[77] S. Dou, C.-L. Dong, Z. Hu, Y.-C. Huang, J.-l. Chen, L. Tao, D. Yan, D. Chen, S. Shen, S. Chou, S. Wang, *Adv. Funct. Mater.* **2017**, *27*, 1702546.

[78] B. Conway, *Solid State Ionics* **2002**, *150*, 93.
[79] N. Mahmood, Y. Yao, J.-W. Zhang, L. Pan, X. Zhang, J.-J. Zou, *Adv. Sci.* **2018**, *5*, 1700464.
[80] R. Miao, B. Dutta, S. Sahoo, J. He, W. Zhong, S. A. Cetegen, T. Jiang, S. P. Alpay, S. L. Suib, *J. Am. Chem. Soc.* **2017**, *139*, 13604.
[81] Q. T. Nguyen, P. D. Nguyen, D. Nguyen, Q. D. Truong, T. T. Kim Chi, T. T. D. Ung, I. Honma, N. Q. Liem, P. D. Tran, *ACS Appl. Mater. Interfaces* **2018**, *10*, 8659.
[82] X.-Y. Yu, L. Yu, H. B. Wu, X. W. D. Lou, *Angew. Chem., Int. Ed.* **2015**, *54*, 5331.
[83] L. Yan, L. Cao, P. Dai, X. Gu, D. Liu, L. Li, Y. Wang, X. Zhao, *Adv. Funct. Mater.* **2017**, *27*, 1703455.
[84] B. Xu, H. Yang, L. Yuan, Y. Sun, Z. Chen, C. Li, *J. Power Souces* **2017**, *366*, 193.
[85] P. Bechtluft, R. G. H. van Leeuwen, M. Tyreman, D. Tomkiewicz, N. Nouwen, H. L. Tepper, A. J. M. Driessen, S. J. Tans, *Science* **2007**, *318*, 1458.
[86] X. Duan, J. Xu, Z. Wei, J. Ma, S. Guo, S. Wang, H. Liu, S. Dou, *Adv. Mater.* **2017**, *29*, 1701784.
[87] J. Wu, S. Ma, J. Sun, J. I. Gold, C. Tiwary, B. Kim, L. Zhu, N. Chopra, I. N. Odeh, R. Vajtai, A. Z. Yu, R. Luo, J. Lou, G. Ding, P. J. A. Kenis, P. M. Ajayan, *Nat. Commun.* **2016**, *7*, 13869.
[88] J. Wu, R. M. Yadav, M. Liu, P. P. Sharma, C. S. Tiwary, L. Ma, X. Zou, X.-D. Zhou, B. I. Yakobson, J. Lou, P. M. Ajayan, *ACS Nano* **2015**, *9*, 5364.
[89] P. P. Sharma, J. Wu, R. M. Yadav, M. Liu, C. J. Wright, C. S. Tiwary, B. I. Yakobson, J. Lou, P. M. Ajayan, X.-D. Zhou, *Angew. Chem., Int. Ed.* **2015**, *54*, 13701.
[90] X. Wang, Z. Chen, X. Zhao, T. Yao, W. Chen, R. You, C. Zhao, G. Wu, J. Wang, W. Huang, J. Yang, X. Hong, S. Wei, Y. Wu, Y. Li, *Angew. Chem., Int. Ed.* **2018**, *57*, 1944.
[91] R. Jasinski, *Nature* **1964**, *201*, 1212.
[92] J. Masa, W. Xia, M. Muhler, W. Schuhmann, *Angew. Chem., Int. Ed.* **2015**, *54*, 10102.
[93] C. C. Page, C. C. Moser, X. Chen, P. L. Dutton, *Nature* **1999**, *402*, 47.
[94] S. Ma, G. A. Goenaga, A. V. Call, D.-J. Liu, *Chem. - Eur. J.* **2011**, *17*, 2063.
[95] J. Tang, R. R. Salunkhe, H. Zhang, V. Malgras, T. Ahamad, S. M. Alshehri, N. Kobayashi, S. Tominaka, Y. Ide, J. H. Kim, Y. Yamauchi, *Sci. Rep.* **2016**, *6*, 30295.
[96] P. Yin, T. Yao, Y. Wu, L. Zheng, Y. Lin, W. Liu, H. Ju, J. Zhu, X. Hong, Z. Deng, G. Zhou, S. Wei, Y. Li, *Angew. Chem., Int. Ed.* **2016**, *55*, 10800.
[97] L. Lai, J. R. Potts, D. Zhan, L. Wang, C. K. Poh, C. Tang, H. Gong, Z. Shen, J. Lin, R. S. Ruoff, *Energy Environ. Sci.* **2012**, *5*, 7936.
[98] A. Aijaz, J. Masa, C. Rösler, W. Xia, P. Weide, R. A. Fischer, W. Schuhmann, M. Muhler, *ChemElectroChem* **2017**, *4*, 188.
[99] X. Fang, L. Jiao, S.-H. Yu, H.-L. Jiang, *ChemSusChem* **2017**, *10*, 3019.
[100] L. Jiao, G. Wan, R. Zhang, H. Zhou, S.-H. Yu, H.-L. Jiang, *Angew. Chem., Int. Ed.* **2018**, *57*, 8525.
[101] Z. Wei, Y. Zhang, S. Wang, C. Wang, J. Ma, *J. Mater. Chem. A* **2018**, *6*, 13790.
[102] E. Skúlason, V. Tripkovic, M. E. Björketun, S. Gudmundsdóttir, G. Karlberg, J. Rossmeisl, T. Bligaard, H. Jónsson, J. K. Nørskov, *J. Phys. Chem. C* **2010**, *114*, 18182.
[103] N. C. Jeong, B. Samanta, C. Y. Lee, O. K. Farha, J. T. Hupp, *J. Am. Chem. Soc.* **2012**, *134*, 51.
[104] J. K. Nørskov, J. Rossmeisl, A. Logadottir, L. Lindqvist, J. R. Kitchin, T. Bligaard, H. Jónsson, *J. Phys. Chem. B* **2004**, *108*, 17886.
[105] J. Barber, *Nat. Plants.* **2017**, *3*, 17041.